Technique for measurement of the noise of a sensor in the presence of large background signals

Aaron Barzilai
Department of Mechanical Engineering, Stanford University, Stanford, California 94305

Tom VanZandt
Center for Space Microelectronics Technology, Jet Propulsion Laboratory MS302-231, 4800 Oak Grove Drive, Pasadena, California 91109

Tom Kenny
Department of Mechanical Engineering, Stanford University, Stanford, California 94305

(Received 3 November 1997; accepted for publication 17 February 1998)

This work reports on a method to measure the instrumental noise of a sensor in the presence of large background signals, based on measuring the coherence and output of two identical sensors exposed to the same input stimulus. The technique can be applied to any sensor characterization problem where there is interest in distinguishing random noise from common-mode noise. The method is demonstrated using geophones, a single-axis seismometer that has been an important sensor for geophysical measurements for decades. Previous experimental work has not published measurements of the geophone's instrumental noise at frequencies near the geophone's resonance because of the presence of large background seismic signals compared to the predicted instrumental noise, which is a minimum at the geophone's resonant frequency. With this coherence technique, measurements performed in the presence of 1 $\mu g/\sqrt{\text{Hz}}$ seismic signals showed that the minimum instrumental noise was within a factor of 2 of the predicted minimum noise of 0.6 $ng/\sqrt{\text{Hz}}$.
 [S0034-6748(98)02305-3]

I. INTRODUCTION

Development of high performance sensors relies heavily on careful characterization of the instrument's behavior. A comprehensive understanding of the error signals in the sensor is the first step towards reducing the errors. Typical sources of spurious signals include thermal noise, mechanical relaxation of packaging, and circuit noise. Measuring these error signals can be quite difficult in the case of high performance sensors, as the error signals they produce are generally orders of magnitude smaller than fluctuations the sensor will see in a laboratory environment.

Seismic instrumentation is an example of a field with this problem, as researchers have produced sensors with instrumental noise levels well below the level of typical background seismic signals. To measure the instrumental noise of these sensors, researchers often take extreme measures to test their sensors in seismically quiet areas. In this article, we present a method to evaluate sensor noise in an environment with large background signals. This technique is demonstrated with geophones, an affordable seismic sensor.

Geophones are highly sensitive ground motion transducers that have been used by seismologists and geophysicists for decades.[1] Figure 1 shows both a schematic drawing and a cross-sectional view of a geophone, which uses the motion of a spring supported coil in the field of a permanent magnet to generate an output signal. Studies of local and regional seismicity often rely on geophones. However, these sensors are most commonly used as sensors for seismic reflection and refraction surveys, techniques to image the three-dimensional structure of oil and gas deposits beneath the Earth's surface. For imaging applications, large, two-dimensional arrays of sensors are deployed on the surface to record seismic waves as they propagate below the ground. By measuring travel times and amplitudes of various components of the waves, the underground structures encountered by the waves can be determined.

Rodgers[2] and Riedesel *et al.*[3] both studied seismometer noise. Riedesel *et al.*[3] developed a model of the noise in a geophone system, including noise in both the geophone and the operational amplifier used for signal processing. This model was experimentally verified by measuring the output of the geophone system and comparing its output to a Streckeisen STS-1 seismometer, considered state of the art for low noise seismometers. The results of Riedesel *et al.*[3] demonstrate the two instruments measured the same motion over the frequency range predicted by the model. Outside this range, the model correctly predicts that the geophone system noise equivalent acceleration (NEA) is greater than the accelerations measured by the STS-1. Riedesel *et al.*[3] use this model to predict the expected NEA of various combinations of geophone models and operational amplifiers. Rodgers[2] performed a similar analysis for a different circuit architecture, enhancing the noise model by accounting for the contribution of forces on the proof mass caused by the current noise through the coil. These forces are significant close to the resonant frequency of a geophone.

In this work, the instrumental noise of a geophone sys-

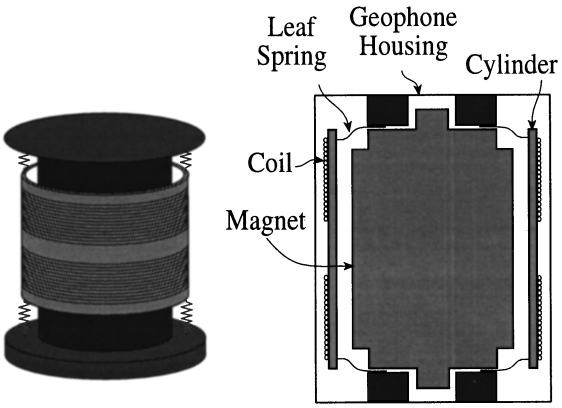

FIG. 1. Schematic drawing and cross-sectional view of a geophone.

tem similar to both Rodgers[2] and Riedesel *et al.*[3] is measured directly in an environment with seismic signals two orders of magnitude larger than the instrumental noise. To verify this measurement, a prediction of the instrumental noise of the geophone system used in this work is first developed. Then, an expression is derived relating the noise of a sensor to the coherence between two sensors exposed to identical inputs and the measured output of one of the sensors. The basis of this derivation was presented by Peterson *et al.*[4] in a United States Geological Survey (USGS) Open-File Report. This technique can be applied easily to a wide assortment of high performance instruments which can often be dominated by environmental noise sources. The data presented below verify that this is an effective method for measuring instrumental noise in the presence of large background signals.

II. GEOPHONE BACKGROUND

A geophone is a single axis seismometer that measures motion in the direction of its cylindrical axis. In typical near-surface deployments, a geophone is packaged with a conical spike and buried a few inches underground to ensure good coupling to the motion of the Earth. Ground motion causes the hollow cylinder of a geophone to move with respect to the geophone housing. The motion of this cylinder inside the geophone is described by Eq. (1), the transfer function of a second-order mechanical system. Equation (1) expresses the relative position of the proof mass, X_r, for the acceleration applied to a geophone, $\ddot{X}_h$, as a function of frequency, with s representing the angular frequency ω multiplied by j, the square root of -1. The mass m[kg], spring constant k[N/m], and damping constant b[N/(m/s)] define the response of the system.

$$\frac{X_r}{\ddot{X}_h} = \frac{-1}{s^2 + \frac{b}{m}s + \frac{k}{m}}. \tag{1}$$

The cylinder's motion is measured by the interaction of the coil on the cylinder with the magnetic field of the permanent magnet inside the geophone. Faraday's law, shown in Eq. (2), states that the voltage across a coil is equal to the change in flux through the coil with respect to time. In the case of a geophone, the change in flux through the coil versus coil displacement, $\partial\phi/\partial X$, is constant for small displacements. Therefore, the voltage across the coil is directly proportional to the velocity of the coil. Geophone manufacturers typically report the constant of proportionality, G[V/(m/s)], known as the transduction constant or generator constant. Huan and Pater[5] demonstrated that G varies by less than 0.005% as a function of position for displacements on the order of 10% of the maximum displacement

$$V_O = -\frac{\partial\Phi}{\partial t} = -\frac{\partial\Phi}{\partial x}\frac{\partial x}{\partial t} = -G\dot{X}_R = -GsX_R. \tag{2}$$

The transfer function relating output voltage to input acceleration, given in Eq. (3), can be determined by combining Eqs. (1) and (2). Unlike most accelerometers, this transfer function is not constant for signals at frequencies below the resonance, as shown in Fig. 2(a). In Eq. (3) and Fig. 2, the transfer function has been evaluated for a 4.5 Hz GS-11D geophone with the characteristics described in Table I. To avoid this complicated frequency dependence of the sensitivity, seismologists consider the sensitivity of the output to velocity. As stated in Eq. (4) and shown in Fig. 2(b), the sensitivity of the output voltage to input velocity is constant at frequencies above the resonance. As a result, seismologists often express geophone outputs as velocity measurements and discard the information on signals with frequencies below the resonance.[6] However, to enable comparisons with other accelerometers, this article will express results in terms of accelerations. Seismologists often express their data in terms of both velocity and acceleration.

$$\frac{V_O}{\ddot{X}_h} = \frac{Gs}{s^2 + \frac{b}{m}s + \frac{k}{m}} = \frac{31.5s}{s^2 + 18s + 760}, \tag{3}$$

$$\frac{V_O}{\dot{X}_h} = \frac{Gs^2}{s^2 + \frac{b}{m}s + \frac{k}{m}} = \frac{31.5s^2}{s^2 + 18s + 760}. \tag{4}$$

III. NOISE PREDICTION

Figure 3 illustrates the circuit used in this work to characterize the instrumental noise of a 4.5 Hz GS-11D geophone. An operational amplifier, the OP-27, is wired as a noninverting amplifier that buffers and amplifies the signal. The OP-27 was selected for its extremely low noise and is recommended by Riedesel *et al.*[3] for low impedance geophones such as the 380 Ω coil of a 4.5 Hz GS-11D. The circuit multiplies the geophone's output by 101.

Thermomechanical noise of the geophone, voltage and current noise of the OP-27, and Johnson noise of the geophone impedance all contribute to the noise at the output. A block diagram of the geophone system with these input noise

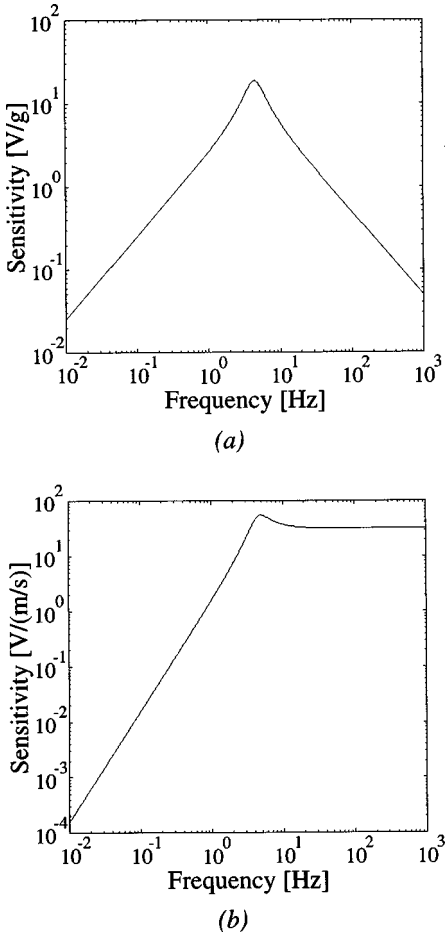

FIG. 2. Predicted sensitivity of an OYO geospace 4.5 Hz GS-11D geophone to (a) acceleration and (b) velocity.

sources is shown in Fig. 4. Many sources of noise in the system are negligible and are not included in the model. Shot noise has a negligible contribution to the system noise. Also, the 10 kΩ and 100 Ω resistors were chosen so that their resistance in parallel produces a negligible amount of Johnson noise.

Since NEA is the square root of the acceleration noise power spectral density (PSD), and the PSDs of incoherent noise sources add, Eq. (5) expresses the total NEA of the geophone system, $\mathrm{NEA}_{\mathrm{Total}}[\mathrm{m/s^2/Hz^{1/2}}]$, where the NEA due to thermal noise of the mechanical system, current noise of the operational amplifier, voltage noise of the operational amplifier, and Johnson noise of the geophone impedance are given by $\mathrm{NEA}_{\mathrm{Thermal}}(\omega)[\mathrm{m/s^2/Hz^{1/2}}]$, $\mathrm{NEA}_{\mathrm{Curr}}(\omega)[\mathrm{m/s^2/Hz^{1/2}}]$, $\mathrm{NEA}_{\mathrm{Volt}}(\omega)[\mathrm{m/s^2/Hz^{1/2}}]$, and $\mathrm{NEA}_{\mathrm{Johnson}}(\omega)[m/s^2/\mathrm{Hz^{1/2}}]$, respectively.

TABLE I. Properties of 4.5 Hz Gs-11D geophone used in experiments

Resonant frequency	4.5 Hz
Damping coefficient	.33
Proof mass	23 g
Sensitivity	32 V/(m/s)
dc coil resistance	380 Ω
case to coil motion	1.8 mm
coil impedance	50 mH
parasitic capacitance	50 pF

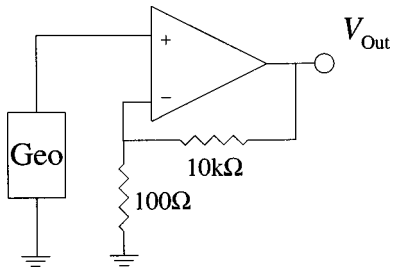

FIG. 3. Sample circuit to measure geophone output.

$$|\mathrm{NEA}_{\mathrm{Total}}(\omega)|^2=|\mathrm{NEA}_{\mathrm{Thermal}}(\omega)|^2+\mathrm{NEA}_{\mathrm{Curr}}(\omega)|^2 +|\mathrm{NEA}_{\mathrm{Volt}}(\omega)|^2+|\mathrm{NEA}_{\mathrm{Johnson}}(\omega)|^2. \tag{5}$$

Equations (6)–(9) give detailed expressions for each of these NEAs. In these equations $k_B[1.38\times10^{-23}\ \mathrm{J/K}]$ is Boltzmann's constant, $T[\mathrm{K}]$ is temperature, $\omega_o[\mathrm{rad/s}]$ is the resonant frequency of the system, and Q is the system's quality factor which is equivalent to $1/(2\zeta)$. $\Delta f[\mathrm{Hz}]$ represents the measurement bandwidth. The NEA due to thermal noise of the mechanical system is given by the well known relation in Eq. (6).[7] $\mathrm{NEA}_{\mathrm{Volt}}(\omega)$ is the operational amplifier's equivalent input voltage noise spectral density (NSD) divided by the geophone's transfer function relating acceleration to voltage, where NSD is the square root of PSD. Operational amplifier current noise passes through the coil producing both an input voltage across the impedance of the geophone, which is treated as an equivalent input voltage NSD, and a force caused by driving current through the coil. Equation (8) gives the expression for $\mathrm{NEA}_{\mathrm{Curr}}(\omega)$, where L represents the geophone's inductance, R the geophone's resistance, and C the parasitic capacitance. Table I contains values for the parameters of a 4.5 Hz GS-11D. The Johnson noise also produces an equivalent input voltage NSD of $\sqrt{4k_BTR\Delta f}$.

$$|\mathrm{NEA}_{\mathrm{Thermal}}(\omega)|=\sqrt{\frac{4k_bT\omega_o\Delta f}{mQ}}, \tag{6}$$

$$|\mathrm{NEA}_{\mathrm{Volt}}(\omega)|=\left|\frac{j\omega+12.5\mathrm{rad/s}}{j\omega}\right|\left(3.2\times10^{-9}\ \frac{\mathrm{V}}{\sqrt{\mathrm{Hz}}}\right) \times\frac{s^2+2\zeta\omega_ns+\omega_n^2}{Gs}, \tag{7}$$

$$|\mathrm{NEA}_{\mathrm{Curr}}(\omega)|\approx\left|\frac{j\omega+12.5\mathrm{rad/s}}{j\omega}\right|\times\left(0.6\times10^{-12}\ \frac{\mathrm{A}}{\sqrt{\mathrm{Hz}}}\right) \times\left(\frac{G}{m}+\frac{Ls+R}{LCs^2+RCs+1}\ \frac{s^2+2\zeta\omega_ns+\omega_n^2}{Gs}\right), \tag{8}$$

$$|\mathrm{NEA}_{\mathrm{Johnson}}(\omega)|=\sqrt{4k_BTR\Delta f}\ \frac{s^2+2\zeta\omega_ns+\omega_n^2}{Gs}. \tag{9}$$

Figure 5 shows the predicted total instrumental noise of the geophone system, expressed as an equivalent input acceleration NSD. The prediction is similar to the noise predictions of Riedesel *et al.*[3] and Rodgers.[2] The minimum noise

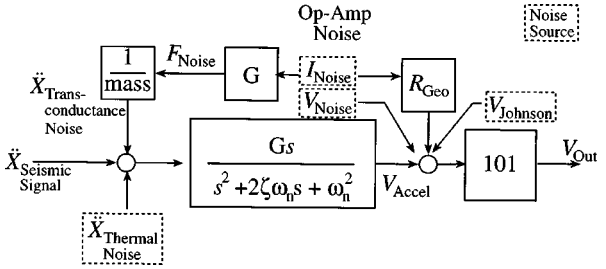

FIG. 4. Block diagram of sample circuit to measure geophone output, including noise sources.

occurs at the resonant frequency, where the sensitivity is greatest. The minimum predicted noise for the system tested in this work is 0.6 ng/$\sqrt{\text{Hz}}$ at 4.5 Hz. The plot also indicates the contribution from each of the noise sources. $\text{NEA}_{\text{Volt}}(\omega)$ is the dominant noise source over most of the frequency range, but near the resonance it dips below $\text{NEA}_{\text{Curr}}(\omega)$ and $\text{NEA}_{\text{Thermal}}(\omega)$.

The USGS Low Noise Model and High Noise Model is also shown on Fig. 5 for reference. It represents the smallest and largest seismic noise measured at seismometer stations across the globe. These stations were selected because of their low seismic noise. Figure 5 illustrates that at the seismically quietest sites in the world, the geophone system tested here is noisier at all frequencies than the seismic signals. This system would not be an appropriate sensor for measuring seismic noise at these stations. At some of the noisier stations, the seismic noise would be larger than the geophone system's instrumental noise, but not the low frequency signals below 0.1 Hz. For low frequency measurements, which can range down to 0.001 Hz, a geophone is not an appropriate sensor. For these applications, a seismometer based on displacement sensing, such as the STS-1 or 2, would be a better choice.[3] In our laboratory at Stanford, one would expect the seismic noise to be on the order of the High Noise Model or greater.

IV. NOISE MEASUREMENT

The noise predictions were tested by measuring the instrumental noise of the geophone system in a first floor laboratory. Since a seismically quiet site was not used, the background seismic signals were much larger than the instrumental noise predictions. To measure the instrumental noise in the presence of large background signals, a technique was employed based on measuring the coherence of the output of two sensors, $\gamma_{XY}^2(\omega)$. Peterson *et al.*[4] first described this technique in the literature.

Coherence can be thought of as the fraction of the power spectrum of signal X that also appears in the power spectrum of signal Y. The coherence between two signals X and Y, $\gamma_{XY}^2(\omega)$ is defined in Eq. (10), where $|G_X(\omega)|$ is the output PSD of signal X, and $|G_{XY}(\omega)|$ is the cross spectral density (CSD) of signal X and signal Y.[8] The PSD and CSD are defined in Eq. (11) and (12), where n_d is the number for records averaged, T is the length of each record, $X_k(\omega,T)$ is the finite Fourier transform of the kth record, and $X_k^*(\omega,T)$ is its complex conjugate. Since both measured signals are accelerations in this work, both spectral densities have units of $[(\text{m/s}^2)^2/\text{Hz}]$

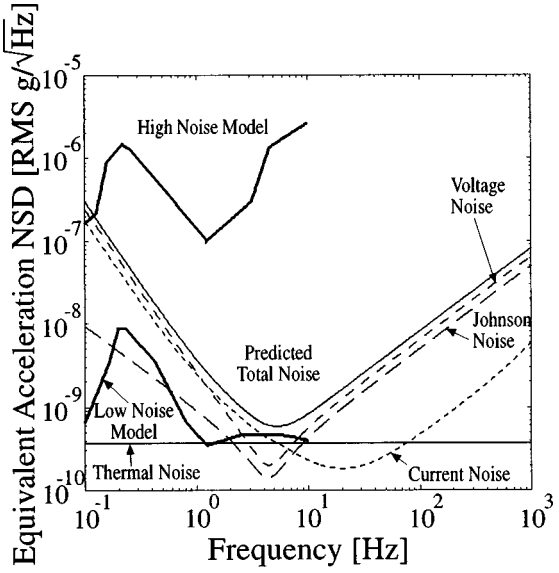

FIG. 5. Predicted noise equivalent acceleration of sample circuit to measure geophone output, and contributions from each source. USGS low and high noise model shown for reference. Results shown are for a 4.5 Hz GS-11D geophone with an OP-27 operational amplifier.

$$\gamma_{XY}^2(\omega)=\frac{|G_{XY}(\omega)|^2}{|G_X(\omega)||G_Y(\omega)|}, \tag{10}$$

$$|G_X(\omega)|=\frac{2}{n_d T}\sum_{n=1}^{n_d}|X_k(\omega,T)|^2, \tag{11}$$

$$|G_{XY}(\omega)|=\frac{2}{n_d T}\sum_{n=1}^{n_d}[X_k^*(\omega,T)][Y_k(\omega,T)]. \tag{12}$$

The coherence and spectral densities of the signals were calculated by the HP89410A vector signal analyzer used to acquire data in this work. Algorithms for computing the coherence between two signals appear in Press *et al.*[9] and Bendat and Piersol.[8]

Figure 6 illustrates a block diagram model of the system used in this work to determine the instrumental noise of a geophone. Two geophones were mounted side by side to ensure that the sensors were exposed to identical acceleration inputs, represented by signal U. This input was caused solely

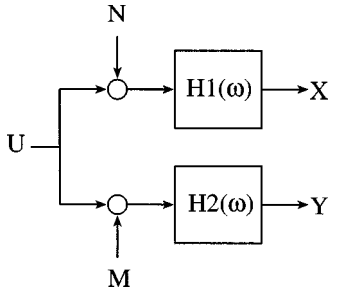

FIG. 6. Block diagram model of experimental system used to measure instrumental noise of a sensor. Signals N and M represent the noise, signals X and Y the measured outputs, and U the input applied to both sensor.

by background seismic signals. Each sensor also has instrumental noise N or M. The total acceleration is then transformed into a voltage by the transfer function of the geophones, recorded by the signal analyzer, and converted into a measured acceleration. Since the acceleration is converted into a voltage and then back to an acceleration, if the conversions are completely accurate then H1 and H2 are equal to 1. In practice they will be linear functions close to 1 but not identical.

For this experiment, each sensor is assumed to have the same magnitude of instrumental noise. Under this condition, Eq. (13) expresses the coherence between the measured outputs. Since the input signal U and the instrumental noise N of the geophone are incoherent, the measured output signal PSD is the sum of the output signal PSD due to the instrumental noise and the output signal PSD due to the input signal, as stated in Eq. (14).

$$\gamma_{XY}^2(\omega)=\frac{1}{1+2\left(\frac{|G_N(\omega)|}{|G_U(\omega)|}\right)+\left(\frac{|G_N(\omega)|}{|G_U(\omega)|}\right)^2}, \tag{13}$$

$$|G_X(\omega)|=|G_N(\omega)|+|G_U(\omega)|. \tag{14}$$

Equation (13) can therefore be simplified to Eq. (15). Equation (16) expresses the relation in terms of NEA, with the NEA of the instrumental noise, $|\mathrm{NEA}_N(\omega)|$, given as a function of the NEA of the measured signal, $|\mathrm{NEA}_X(\omega)|$, and the coherence between the two outputs, $\gamma_{XY}^2(\omega)$

$$|G_N(\omega)|=|G_X(\omega)|[1-\sqrt{\gamma_{XY}^2(\omega)}], \tag{15}$$

$$|\mathrm{NEA}_N(\omega)|=|\mathrm{NEA}_X(\omega)|\sqrt{[1-\sqrt{\gamma_{XY}^2(\omega)}]}. \tag{16}$$

V. RESULTS AND DISCUSSION

Figure 7 illustrates the data collected along with the predicted total noise for reference. The output of one of the geophones is labeled ''Seismic Signal.'' From 2 to 300 Hz this background signal is roughly two orders of magnitude or more greater than the predicted noise. As expected, the coherence between the two output signals (not shown) in this frequency range was greater than 0.999. This indicates that the two sensors are subject to identical input signals, which are caused by seismic noise.

The discontinuity of the seismic signal at 10 Hz occurs because spectrums were taken over multiple frequency ranges to enable good resolution of the instrumental NEA over a wide frequency range. The data above 10 Hz were collected with the geophones on a floating optical table to attenuate the magnitude of the seismic signals. However, the resonance of the table amplified the signal at frequencies near 1 Hz. Therefore, low frequency data was collected with the geophones on the floor.

The instrumental noise was determined from the data via the coherence method described previously and is also plotted in Fig. 7. The measured instrumental noise matches the prediction well, although the data show that the geophone system is roughly a factor of two noisier than predicted.

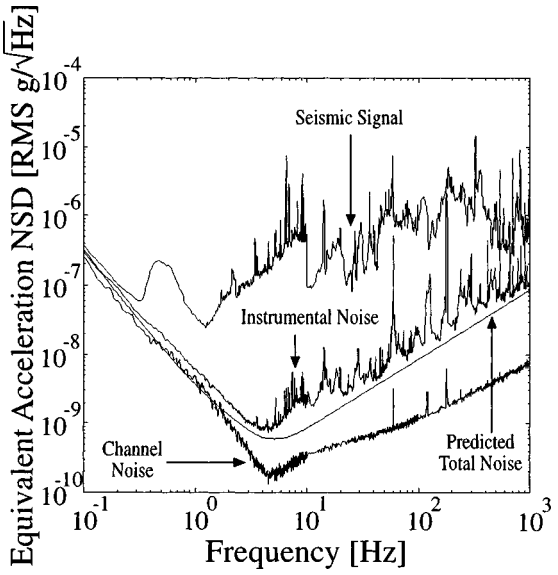

FIG. 7. Predicted and measured noise equivalent acceleration of a 4.5 Hz GS-11D geophone with an OP-27 operational amplifier.

These results clearly demonstrate that the coherence method can be used to measure instrumental noise of a sensor in the presence of large background signals.

The peaks in the instrumental noise are not predicted by the noise model. The coherence must be greater than 0.9998 to enable a measurement of instrumental noise that is two orders of magnitude below the background signal. In the data shown in this work, the coherence rarely exceeded this value. In the frequency ranges where the coherence was at this practical limit, the measured instrumental noise spectrum matched the trends of the background signal. This is to be expected in regions where the coherence is constant. This practical limit was attributed to nonideal coupling between the two geophones.

Errors due to finite resolution in the analog to digital converters of the HP89410A are another possible source of error in this experiment. Although the noise of data recorders can be greater than the noise of the sensors being recorded, that was not the case in this instance. Figure 7 shows that the noise of a channel of the HP89410A, labeled ''Channel Noise,'' is below the measured instrumental noise at all frequencies. In general, the coherence technique will yield the magnitude of the incoherent signal, which is comprised of the instrumental noise and the recorder noise. The PSD of the incoherent signal is the sum of the PSD of the instrumental noise and the PSD of the recorder noise. As long as the magnitude of the recorder noise is known, this technique can be used to extract the instrumental noise of a sensor, even if the instrumental noise is of the same magnitude as the recorder noise. In practice it would be difficult, although not impossible, to measure instrumental noise when it is less than the magnitude of the recorder noise.

ACKNOWLEDGMENTS

This work was supported by the Center for Space Microelectronics Technology, Jet Propulsion Laboratory, California Institute of Technology, and is sponsored by the Na-

tional Aeronautics and Space Administration, Office of Space Access and Technology. The authors also acknowledge the National Science Foundation CAREER Award-(Grant No. ECS9502046), the Charles Lee Powell Foundation, and the Terman Fellowship.

[1] R. E. Sheriff and L. P. Geldart, *Exploration Seismology*, 2nd. ed. (Cambridge University Press, New York, 1995), pp. 6–13.
[2] P. W. Rodgers, Bull. Seismol. Soc. Am. **84**, 222 (1994).
[3] M. Riedesel, R. D. Moore, and J. A. Orcutt, Bull. Seismol. Soc. Am. **80**, 1725 (1990).
[4] J. Peterson, C. R. Hutt, and L. G. Holcomb, ''Test and Calibration of the Seismic Research Observatory,'' United States Geological Society Open-File Report 80-187.
[5] S. L. Huan and A. R. Pater, Geophysics **50**, 1221 (1985).
[6] M. B. Dobrin, *Introduction to Geophysical Prospecting*, 3rd. ed. (McGraw-Hill, New York, 1976), p. 63.
[7] M. J. Usher, I. W. Buckner, and R. F. Burch, J. Phys. E: Sci. Instrum. **10**, 1250 (1977).
[8] J. S. Bendat and A. G. Piersol, *Engineering Applications of Correlation and Spectral Analysis*, 2nd ed. (Wiley, New York, 1993).
[9] W. H. Press, S. A. Teukolsky, W. T. Vetterling, and B. P. Flannery, *Numerical Recipes in C*, 2nd ed. (Cambridge University Press, Cambridge, 1992), pp. 549–558.